Expedient decagram-scale synthesis of robust organic cages that bind sulfate strongly and selectively in water

Émer M. Foyle,[1] Rosemary J. Goodwin,[1] Cameron J. T. Cox,[1,2] Bailee R. Smith,[1] Annie L. Colebatch,[1] and Nicholas G. White[1,3]*

[1]Research School of Chemistry, The Australian National University, Canberra, ACT, Australia

[2]EaStCHEM School of Chemistry, The University of Edinburgh, Edinburgh, Scotland, UK

[3]Lead contact

*Correspondence: nicholas.white@anu.edu.au

Selective anion recognition remains a key challenge in supramolecular chemistry: only a very small number of systems that can function in water are known, and these nearly always preferentially bind hydrophobic anions. In this work, we report three robust hexa-cationic cages that can be prepared on scales up to 14 g in two simple and high-yielding steps from commercially-available materials. One of these cages displays unusually strong sulfate binding in water (K_a = 12,000 M^{-1}), and demonstrates high selectivity for this anion over $H_2PO_4^-$/HPO_4^{2-} in DMSO/buffer mixtures. These results demonstrate that relatively large, three-dimensional supramolecular hosts can be prepared in high yields and on large scales, and can be highly potent receptors.

INTRODUCTION

One of the major challenges in the field of supramolecular anion recognition is to achieve selective recognition in water to facilitate a range of biological, environmental and industrial applications.[1–3] Water is an inherently competitive solvent that can interact favourably with both receptors and anions, which have notoriously high solvation energies, however functioning in water is absolutely necessary for nearly all proposed applications. While there have been notable examples of receptors that can function in neutral water,[4–12] the majority of receptors are unable to do so. Furthermore, in addition to difficulties binding anions in water, achieving selectivity remains a Herculean challenge. Systems have been reported that display a selectivity preference for more highly charged anions over those with a lower charge,[13,14] or based on anion hydrophobicity,[4,15] but systems that show significant selectivity between similar anions such as SO_4^{2-} and HPO_4^{2-} are extremely rare.[12,16–18] A notable exception is a very recent report from Deplazes, Wu and co-workers who showed that neutral urea-based cage **1** could achieve selective SO_4^{2-} recognition, with an association constant of 66 M^{-1} in water, and 990 M^{-1} in a micelle-based system (Figure 1).[12] A recent pre-print from the same group has reported new cages that can bind sulfate even more strongly, with association constants of up to 8,400 M^{-1}.[19]

Many of the anion receptors that are capable of functioning in competitive media take advantage of a complex 3D architecture to encapsulate the guest, with prominent examples including interlocked catenanes/rotaxanes[20–22] and organic cage molecules.[23–31] The well-defined internal cavity in these systems offers the potential to isolate an anion from a competitive solvent, as well as achieving size and shape-based selectivity, but even then *selective* anion recognition in media containing a significant amount of water is very unusual. Additionally, preparing complex 3D receptors often requires lengthy multistep syntheses and difficult purification, with the consequence that many high-performing hosts are typically only prepared on the milligram scale.

In order to make these kinds of 3D hosts on larger scales, it would be ideal to use dynamic covalent chemistry as this incorporates an “error checking” process that arises from the reversibility of the reaction. The imine formation reaction is the most popular choice and has been used to prepare a range of cages[32–35] and interlocked molecules,[36–39] and in some cases imine cages have been prepared on impressively large scales.[40,41] While imines have proved useful, they are often (but not always[42–45]) hydrolytically unstable in water and this limits their use in many applications including anion recognition in aqueous media. One approach to overcome this is to form a cage by imine bond formation and then to use an additional reaction to convert the imine bonds to a more robust linkage,[35,46–48] and a notable example of this approach on a 2.1 g scale was recently reported by Andrews.[49]

Hydrazones are structurally similar to imines and can be prepared using reversible reactions in water, usually in the presence of an acid catalyst.[50] The hydrazone formation reaction has been used to synthesise macrocycles,[51–53] interlocked structures,[54–58] and knots,[59] and a small number of hydrazone cages have been reported in the last decade.[60–64] More recently, Schneebeli demonstrated that a hydrazone cage could be prepared on a 2.6 g scale

over eight steps.[65] Typically hydrazone formation is reversible in the presence of acid and heat, meaning that it potentially offers the best of both worlds in that it is reversible under the reaction conditions leading to error correction, but largely irreversible in most other conditions, resulting in more robust products.

The ease of synthesis of hydrazone cages, coupled with their potentially high stability, makes them an attractive candidate for use as anion receptors. Well-defined three-dimensional cavities for selective anion recognition could potentially be prepared quickly in high yield. Indeed, Li and Sessler have reported the hydrazone cage $\mathbf{2}^{6+}$,[63] which binds two anions simultaneously in the polar organic solvent acetonitrile and forces them within van der Waals radii of each other, while Li has used hydrazone self–assembly to prepare cage $\mathbf{3}^{6+}$ that can bind iodide strongly in water (K_a = 4,300 M^{-1}). The cage shows a selectivity for this halide over more hydrophilic anions,[28] presumably due to its lower hydration energy (ΔG_{hyd} for I^- = –275 kJ mol^{-1}, ΔG_{hyd} for Cl^- = –340 kJ mol^{-1}; for comparison, ΔG_{hyd} for SO_4^{2-} = –1080 kJ mol^{-1}).[66]

In this report, we describe the synthesis of robust hydrazone cages in a simple two-step procedure from commercially-available reagents, including the preparation of one on a 14 g scale. Purification is by simple precipitation in both steps. We show that the resulting cages can bind sulfate remarkably strongly and selectively in water, thus demonstrating that it is possible to recognise anions selectively in water with readily-preparable hosts.

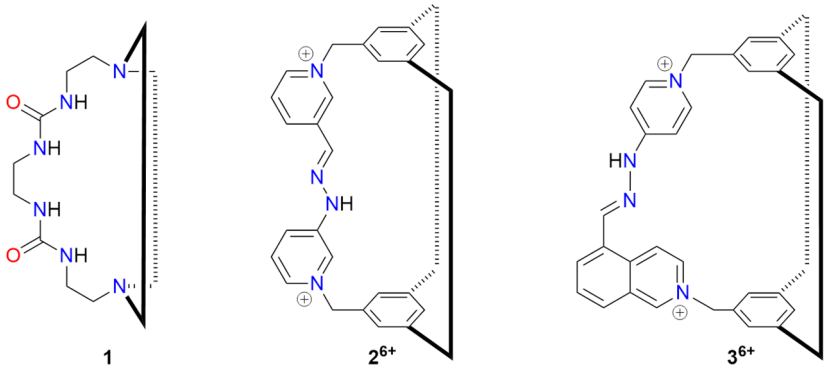

Figure 1. Previously-reported anion binding cages relevant to this work.

Compound **1** was reported by Deplazes, Wu and co-workers and binds sulfate in water;[12] compound $\mathbf{2}^{6+}$ was reported by Li and Sessler and binds two anions closer than the sum of their van der Waals radii in acetonitrile;[63] $\mathbf{3}^{6+}$ was reported by Li and binds iodide in water.[28] In all cases, only one "arm" of each cage is shown, with the others simplified to bold or dotted lines.

RESULTS AND DISCUSSION

Synthesis of cages

The cages were synthesized through a simple two-step process. Reaction of commercially-available tris(bromomethyl) species **4** and 4-pyridinecarboxaldehyde in DMF gave pure $\mathbf{5}\cdot\mathbf{Br_3}$ in very high yield (Scheme 1). The initially isolated solid contains a mixture of aldehyde and hydrated gem-diol form. However, simply suction-drying the compound in air for several hours resulted in essentially complete conversion of the aldehydes to gem-diols (see SI for extensive studies optimising the preparation of $\mathbf{5}\cdot\mathbf{Br_3}$). Using the optimised procedure, $\mathbf{5}\cdot\mathbf{Br_3}$ can be readily and reproducibly prepared on a 12 g scale in 96% yield. With this key hydrated tris-aldehyde building block in hand, we subsequently investigated the synthesis of cages from this and dihydrazides. We selected the three hydrazides **6** – **8**, of which **6** and **7** are commercially-available (and inexpensive); **8** is commercially-available but is expensive, and so was readily prepared from the reaction of the analogous ester and hydrazine hydrate.[67]

Initial studies of cage formation were conducted on NMR scales by heating D_2O solutions containing 4.0 mM of $\mathbf{5}\cdot\mathbf{Br_3}$ and 6.0 mM of the appropriate dihydrazide at 80 °C. In all cases, significant amounts of cage formation were observed: in the case of $\mathbf{cage}^{\mathbf{urea\ 6+}}$, the cage was the major product but significant amounts of other products were also observed. Adding an acid catalyst increased the amount of $\mathbf{cage}^{\mathbf{urea\ 6+}}$ formed, such that it was the dominant product in solution (> 90% based on integration of the ^1H NMR spectra). In the cases of $\mathbf{cage}^{\mathbf{ph\ 6+}}$ and $\mathbf{cage}^{\mathbf{py\ 6+}}$, the cages were the dominant products in solution (> 90%) whether or not an acid catalyst was used. Interestingly, the cages also formed at room temperature in D_2O without the addition of a catalyst, although this was very sluggish (months).

We next investigated preparative scale reactions to form the cages. If these reactions were conducted at relatively low concentrations (4.0/6.0 mM of $\mathbf{5}\cdot\mathbf{Br_3}$/dihydrazide), all material stayed dissolved and then high yields of cages could be isolated by adding NH_4PF_6 to precipitate the PF_6^- salts of the cages. This gave high yields of cages (typically ~ 70%), with reasonably high purity (typically 90 – 95% purity), although it was difficult to further purify the cages.

Instead we found that by carefully selecting reaction concentrations, it was possible to find conditions where the starting materials were soluble but the cages precipitated from solution during the reaction as the bromide salts. While the bromide salts of these cages do dissolve in water, their solubility is low enough (1 – 3 mM) that significant yields of precipitated cages can be isolated. Using this approach, very high purity cages were obtained and were isolated by simple filtration and washing (^{1}H NMR spectra are shown in Figure 2).

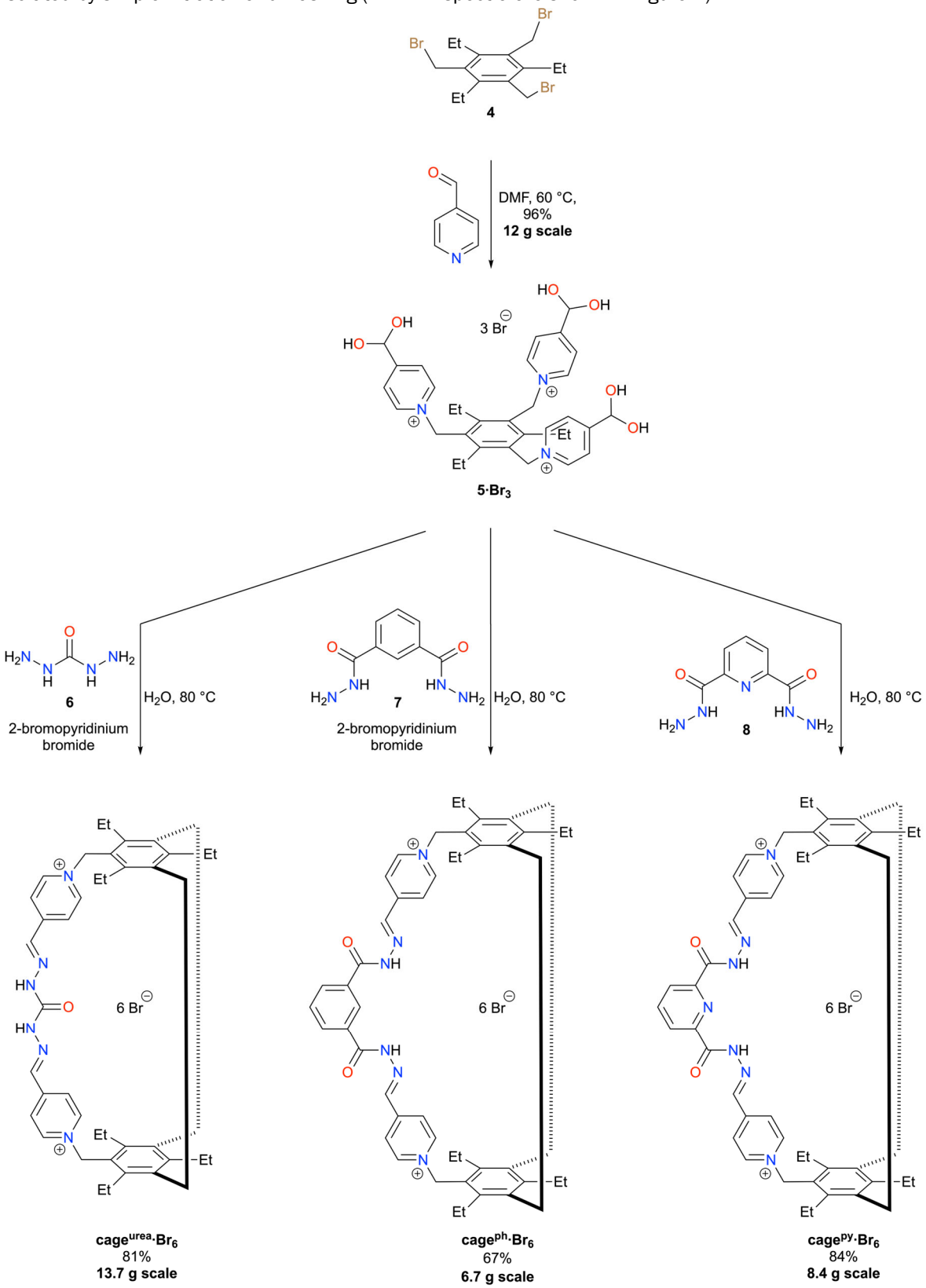

Scheme 1. Multi-gram synthesis of hydrazone cages.

In all cases, only one "arm" of each cage is shown, with others simplified to bold or dotted lines.

In the case of **cage^{py}·Br$_6$**, this reaction proceeded smoothly without addition of a catalyst and it was possible to prepare this cage on a large scale and in good yield (8.4 g, 84%). Conducting the reactions to form **cage^{urea}·Br$_6$** and **cage^{ph}·Br$_6$** without acid did result in precipitation of clean product after optimisation of reaction concentration, however yields were relatively low (~ 50 and 30%, respectively). We therefore investigated the use of acid catalysts to improve the yield. Typically, trifluoroacetic acid (TFA) is used as a catalyst in these kinds of hydrazone formation reactions,[50] and we found that it does indeed improve product formation in NMR-scale, low concentration reactions (SI). However, it is not ideal in this case due to the likelihood of forming mixed trifluoroacetate/bromide salts of the cages. We instead studied the use of 2-bromopyridinium bromide, *i.e.* the HBr adduct of 2-bromopyridine, as the *p*K_a of this salt is similar to TFA.[68,69] This compound is a crystalline salt and can be conveniently prepared on multi-gram scales from 2-bromopyridine and HBr$_{(aq)}$ (see SI). Adding catalytic amounts of 2-bromopyridinium bromide to the reactions to form **cage^{urea}·Br$_6$** and **cage^{ph}·Br$_6$** resulted in precipitation of clean cage products in good yields (^{1}H NMR spectra of all three as-isolated cages are shown in Figure 2A).[70] These reactions were amenable to scale-up, and we were able to prepare **cage^{ph}·Br$_6$** on a 6.7 g scale in 67% isolated yield, and **cage^{urea}·Br$_6$** on a 13.7 g scale in 81% isolated yield.

Pleasingly, we have not observed any reduction in yield upon increasing reaction scale, and we are confident that even larger scale preparations would be similarly easy. The conditions reported give multiple grams of all cages in two steps from commercially-available materials and the reactions are operationally simple with no purification needed beyond filtering and washing the precipitated products. All three cages were characterised by ^{1}H and ^{13}C{^{1}H} NMR spectroscopy, high resolution mass spectrometry, X-ray crystallography and DOSY NMR spectroscopy, which gave diffusion coefficients consistent with the expected size of the cages.

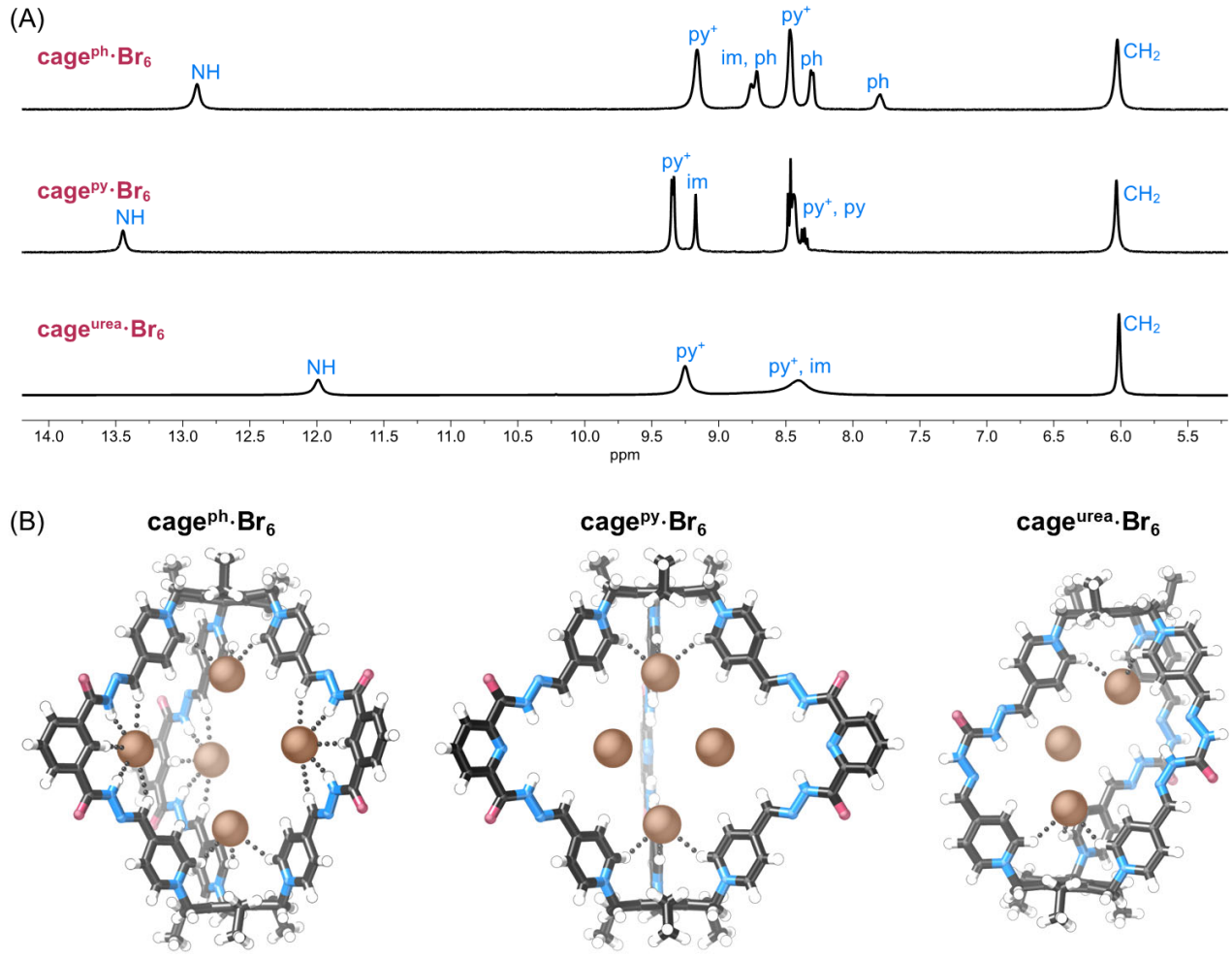

Figure 2. Characterisation of hydrazone cages.

(A) Partial ^{1}H NMR spectra of cages; labelling: py$^+$ = pyridinium, py = pyridyl, ph = phenyl, im = imine (d$_6$-DMSO, 400 MHz, 298 K).
(B) X-ray crystal structures of **cage^{ph}·Br$_6$**, **cage^{py}·Br$_6$** and **cage^{urea}·Br$_6$**; only Br$^-$ anions located inside the cage cavity are shown, a dotted line indicates a close contact shorter than the van der Waals' radii of H and Br. Disorder is omitted for clarity, PLATON-SQUEEZE[73] or OLEX2[74] mask feature was used in all cases.

We were able to obtain crystals of **cage^{ph}·Br$_6$**, **cage^{py}·Br$_6$** and **cage^{urea}·Br$_6$** suitable for X-ray diffraction experiments (Figure 2B, several crystal structures of other salts of the cages were also obtained and are presented in Figure 4 and the SI). The single crystal structures of these cages show considerably different cage shapes. **Cage^{urea}·Br$_6$** is relatively compact, and takes on a "buckled" geometry, resulting in a relatively small cavity (~ 6 Å across). In contrast, **cage^{ph}·Br$_6$** and **cage^{py}·Br$_6$** have much larger cavities (~ 15 Å at the widest part). In the case of **cage^{py}·Br$_6$**, this appears to be aided by N–H···N hydrogen bonds between hydrazone N–H groups and the pyridine nitrogen atom preorganising this part of the molecule.[71] In some cases, there appears to be more than one possible position for some of the bromide anions, but in all structures bromide anions sit in both of the pockets formed from three pyridinium rings, with each anion receiving two or three C–H···Br$^-$ hydrogen bonds (H···Br$^-$ distances: 2.66 – 3.05 Å, 86 – 100% of the sum of van der Waals radii[72]). We were able to obtain a crystal structure of **cage^{urea}·Cl$_6$** (SI), and interestingly in this structure only two chloride anions are located inside the cage, where they hydrogen bond to urea N–H donors, with the remainder outside of the cage cavity. While these are solid state structures so may not be representative of solution behaviour, it is interesting to note that Cl$^-$ anions are not located in the pyridinium pockets, which may be related to observed preferential solution phase binding of Br$^-$ over Cl$^-$ to the cage (see later).

Stability of cages

Given the facile preparation of the cages (including in water at room temperature), we were worried that they may be prone to degradation/rearrangement. We therefore tested the stability of the cages to a range of stimuli and in a range of solvents. Full details are given in the SI, but in short, it appears the cages are surprisingly stable. **Cage^{ph}·Br$_6$** and **cage^{py}·Br$_6$** do not show significant degradation even after heating at 80 °C for seven days in D_2O, d_6-DMSO or in acidic buffer (acetic acid/acetate buffer, pH = 4.0). Studies in basic buffer could not be conducted for these cages due to limited solubility. Urea cage **cage^{urea}·Br$_6$** does not show any observable degradation on prolonged standing (14 days) at room temperature in either D_2O or d_6-DMSO, or in the presence of acidic (acetic acid/acetate buffer, pH = 4.0), neutral (tris buffer, pH = 7.2) or basic buffer (borate buffer, pH = 10.5). Minor degradation (~ 1 – 2% per day) is observed upon heating at 80 °C in water, DMSO, or acidic buffer, while degradation upon heating at 80 °C in basic buffer is more rapid (~ 50% degradation after 24 hours). The cages decompose in strongly acidic or basic conditions (pH = 1, 14), although we do not think this will be an issue for any likely uses of the cages.

NMR and ITC solution anion binding studies

Initial sulfate binding studies in 1:1 D_2O:d_6-DMSO

All three cages have 6$^+$ charges and contain potential C–H hydrogen bond donors from the cationic pyridinium rings as well as amide N–H groups. We therefore studied the anion recognition properties of the cages, initially as their bromide salts. We first studied the binding of SO_4^{2-} to all three cages using ^{1}H NMR titration experiments in 1:1 D_2O:d_6-DMSO, as this is a highly competitive solvent and all cages have high solubility in this mixture. Addition of sulfate results in downfield shifts of C–H resonances (Figure 3): in the case of **cage$^{urea\ 6+}$**, the largest shifts occur for the pyridinium resonance *meta* to the nitrogen atom. In the case of **cage$^{ph\ 6+}$** and **cage$^{py\ 6+}$**, negligible shifts are observed for the pyridinium peaks, or the external phenylene/pyridine peaks, but relatively large shifts are observed for the imine peak, and in the case of **cage$^{ph\ 6+}$**, the internal phenylene C–H resonance. Fitting the imine peak movements to 1:1 binding isotherms using *Bindfit*[75] revealed moderately strong binding for **cage$^{ph\ 6+}$** and **cage$^{py\ 6+}$** (K_a = 690 ± 90 and 280 ± 10 M^{-1}, respectively, Table 1; these and all subsequent ± values represent 95% confidence intervals). In contrast, **cage$^{urea\ 6+}$** appears to bind SO_4^{2-} very strongly, although it was difficult to quantify binding at 298 K in this solvent mixture due to the NMR peaks broadening and becoming inequivalent upon anion addition (Figure 3A). Given that almost no movement of peaks is observed after addition of one equivalent of anion, we believe that the association constant is > 10^4 M^{-1}. To obtain more reliable association constants, we repeated the study of sulfate binding to **cage$^{urea\ 6+}$** at 333 K as peaks are relatively sharp and in fast exchange at this temperature. This experiment confirmed that K_a was indeed > 10^4 M^{-1}.

Presumably **cage$^{urea\ 6+}$** binds more strongly than the larger phenyl and pyridyl cages as its smaller size can effectively protect the anion from bulk solvent, while holding it relatively close to the six positive charges from the pyridinium rings. This is consistent with ^{1}H NMR experiments where the pyridinium peaks moving significantly, and is supported by X-ray crystallographic analysis, see later. In contrast, the larger sizes of **cage$^{ph\ 6+}$** and **cage$^{py\ 6+}$** mean that the anion can "rattle around" in the cage, and binding appears to occur more at the central phenyl/pyridyl part of the cage.

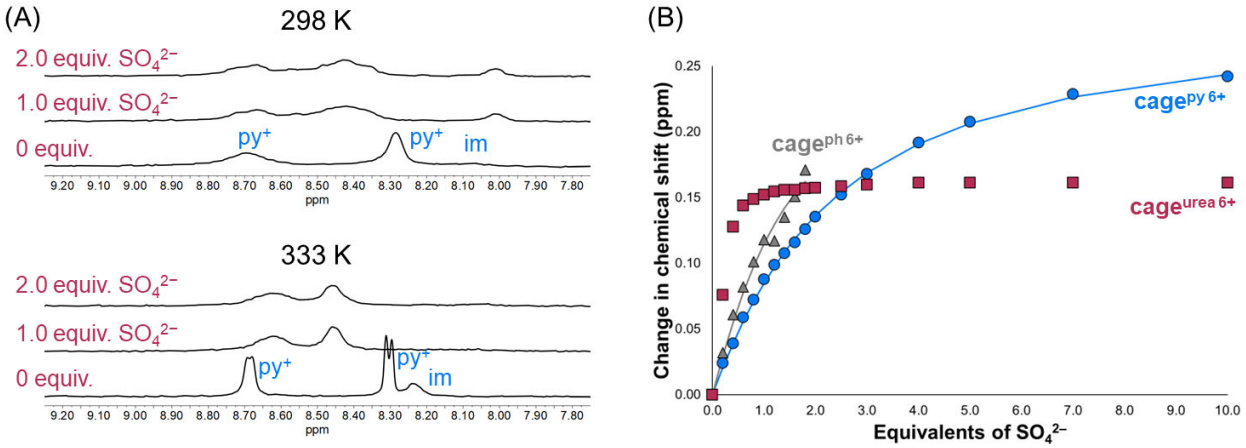

Figure 3. ^{1}H NMR shifts upon sulfate binding.

(A) Partial ^{1}H NMR spectra of **cage^{urea}·Br$_6$** upon addition of SO_4^{2-} at 298 K and 333 K showing significant peak broadening at 298 K (1.0 mM in cage, 400 MHz, 1:1 D_2O:d_6-DMSO). Digital de-noising has been applied to the spectra (see SI Section 4.1).
(B) Movement of imine or pyridinium resonances upon addition of SO_4^{2-} to cages in 1:1 D_2O:d_6-DMSO. Imine peak was followed for **cage$^{ph\ 6+}$** and **cage$^{py\ 6+}$**, pyridinium peak was followed for **cage$^{urea\ 6+}$**. Different peaks were followed for different cages as these showed the largest changes, which we attribute to different anion binding locations (see SI for more details). Data for **cage$^{ph\ 6+}$** and **cage$^{py\ 6+}$** were recorded at 298 K, data for **cage$^{urea\ 6+}$** were recorded at 333 K. Points represent observed data, lines represent fitted 1:1 isotherms calculated in *Bindfit*;[75] no isotherm could be determined for **cage$^{urea\ 6+}$** as binding was too strong to quantify by ^{1}H NMR titration experiments. **Cage$^{ph\ 6+}$** precipitated at 2.5 equivalents of anion.

Table 1. Sulfate association constants for cage^{ph}·Br$_6$, cage^{py}·Br$_6$ and cage^{urea}·Br$_6$ determined by ^{1}H NMR titration experiments in 1:1 D_2O:d_6-DMSO.

Host	Temp. (K)	K_a (M^{-1})
Cage^{ph}·Br$_6$	298	690 ± 90
Cage^{py}·Br$_6$	298	280 ± 10
Cage^{urea}·Br$_6$	298	strong[a]
Cage^{urea}·Br$_6$	333	> 10^4

Association constants calculated using *Bindfit*,[75] the ± value represents the asymptotic error[76] at the 95% confidence interval.
[a] Due to peak broadening and desymmetrisation upon addition of SO_4^{2-} to **cage$^{urea\ 6+}$** at 298 K, it was not possible to determine accurate association constants at this temperature. Qualitatively, binding appears to be very strong (> 10^4 M^{-1}), as evidenced by little change in the ^{1}H NMR spectrum after addition of more than one equivalent of anion.

Binding of sulfate to cage$^{urea\ 6+}$ in water

Based on our initial studies that showed that **cage$^{urea\ 6+}$** binds sulfate much more strongly than the other two cages, we focused on this cage for more detailed investigation, and conducted these experiments in water. ^{1}H NMR titration experiments were conducted in D_2O at 333 K to give sharp peaks that could be followed reliably, and we also conducted isothermal calorimetry (ITC) studies in H_2O at 298 K. The X-ray crystal structure of **cage^{urea}·Br$_6$** (Figure 2B) suggests the possibility of favourable interactions between the cage and Br^- anions, so we attempted to measure the extent of this interaction in solution. A dilution experiment[77] was conducted to quantify the extent of ion-pairing in **cage^{urea}·Br$_6$** in D_2O and this revealed a $K_{ion\ pairing}$ for bromide of 4,800 ± 200 M^{-1} in D_2O at 333 K. This value suggests quite strong interactions between Br^- and the "free" cage, although in itself is not particularly meaningful as free cage cannot be physically obtained. We therefore prepared other salts of **cage$^{urea\ 6+}$**, namely the PF_6^-, Cl^- and NO_3^- salts using simple and high-yielding precipitation reactions (see SI). We conducted quantitative NMR titration experiments to determine Br^- binding to **cage^{urea}·Cl$_6$** and **cage^{urea}·(NO$_3$)$_6$** in D_2O (**cage^{urea}·(PF$_6$)$_6$** did not have sufficient solubility to conduct these experiments). While values are relatively inexact due to small peak shifts in this competitive solvent (see SI), K_a values Br^- relative to Cl^- and NO_3^- were measured as 250 ± 25 and 87 ± 9 M^{-1}, respectively (Table 2). Stronger binding of Br^- than Cl^- in water is expected based on the relative hydration energies of the anions,[66] although it is interesting that Br^- binds more strongly than less hydrophilic NO_3^-. We suspect that this arises because Br^- can fit close to all three cationic pyridinium groups, while larger NO_3^- cannot.

Quantitative NMR titration experiments at 333 K revealed strong sulfate binding to **cage^{urea}·Br$_6$** in D_2O, with a K_a value of 9,600 ± 2,600 M^{-1}. Given that sulfate has to compete with the presence of six equivalents of bromide, which itself can bind to the cage, this value is likely a significant underestimate. Indeed accounting for ion pairing, we can estimate the binding of sulfate to the free cage as approximately 260,000 M^{-1} (See SI 4.5.5), although we note this value has little practical meaning. To determine sulfate affinity in water more accurately, we conducted

ITC titrations in water at 298 K studying anion binding to **cage^{urea}·Br$_6$** and **cage^{urea}·Cl$_6$** (attempts to measure sulfate binding to **cage^{urea}·(NO$_3$)$_6$** were hampered by precipitation).

ITC determination of sulfate binding to **cage^{urea}·Br$_6$** gave a slightly lower association constant than that estimated from ^{1}H NMR titrations (K_a = 3600 ± 600 M^{-1}), although we note that the values were recorded at different temperatures (333 K for NMR experiments, 298 K for ITC). As expected based on the ^{1}H NMR studies, binding to the chloride salt of **cage$^{urea\ 6+}$** is significantly stronger than binding to the bromide salt (K_a for **cage^{urea}·Cl$_6$** = 12000 ± 3200 M^{-1}). This is a remarkably high association constant for binding a highly hydrophilic anion in water. While the 6+ charge of the cage undoubtedly provides electrostatic attraction for sulfate, it also hinders binding as sulfate recognition has to compete with the halide anions. In both cases, sulfate binding is entropically-driven and slightly enthalpically unfavourable (ΔH = 5.5 ± 0.6 kJ mol^{-1}, −TΔS = −25.7 ± 0.2 kJ mol^{-1} for sulfate binding to **cage^{urea}·Br$_6$**; ΔH = 2.7 ± 0.4 kJ mol^{-1}, −TΔS = −25.9 ± 1.2 kJ mol^{-1} for sulfate binding to **cage^{urea}·Cl$_6$**). The favourable entropy component presumably arises from the release of ordered water molecules from the cage cavity. We note that Kubik has shown that binding of sulfate to a neutral bis-cyclopeptide receptor in water is entropically-driven,[78] and Severin has shown that chloride binding in water by a tetra-cationic Pd(II)-based cage is also enthalpically unfavourable.[10]

Table 2. Sulfate association constants and cage^{urea}·Br$_6$ in water[a] determined by ^{1}H NMR titration experiments.

Host	Guest	Technique	Temp. (K)	K_a (M^{-1})	ΔH (kJ mol^{-1})	−TΔS (kJ mol^{-1})
Cage^{urea}·Cl$_6$	Br$^-$	^{1}H NMR	333	250 ± 25	–	–
Cage^{urea}·(NO$_3$)$_6$	Br$^-$	^{1}H NMR	333	87 ± 9	–	–
Cage^{urea}·Br$_6$	SO$_4^{2-}$	^{1}H NMR	333	9600 ± 2600	–	–
Cage^{urea}·Br$_6$	SO$_4^{2-}$	ITC	298	3600 ± 600	5.5 ± 0.6	−25.7 ± 0.2
Cage^{urea}·Cl$_6$	SO$_4^{2-}$	ITC	298	12000 ± 3200	2.7 ± 0.4	−25.9 ± 1.0

^{1}H NMR titrations were conducted in D_2O; association constants were calculated using *Bindfit*,[75] the ± value represents the asymptotic error[76] at the 95% confidence interval. ITC studies were conducted in H_2O; association constants were calculated using NanoAnalyze,[79] the ± value represents the 95% confidence interval with errors calculated based on the variance in multiple experiments.

Sulfate/hydrogenphosphate selectivity

Cage$^{urea\ 6+}$ binds sulfate very strongly in water while interacting less strongly with monovalent anions. We next attempted to compare the selectivity of **cage$^{urea\ 6+}$** for sulfate with closely-related HPO$_4^{2-}$, however we found that addition of HPO$_4^{2-}$ resulted in deprotonation of **cage$^{urea\ 6+}$**. To usefully compare binding strength without titrations being complicated by guest-induced deprotonation, we next studied binding in tris buffers. Unfortunately, **cage$^{urea\ 6+}$** precipitates upon standing in tris buffers and so titrations were carried out in 1:1 tris buffers:d$_6$-DMSO .The structure of the precipitate obtained from aqueous tris buffer was determined by X-ray crystallography, which showed a very similar cage conformation to that in the crystal of **cage^{urea}·6Br** (see SI). NMR studies in 1:1 tris buffers:d$_6$-DMSO indicated that the cage remained fully protonated when buffer at pH 7.2 or 7.5 was used, but some deprotonation was evident in pH = 8.0 buffer, and significant deprotonation at higher pH values.

In 1:1 pH = 7.2 tris buffer:d$_6$-DMSO, sulfate binding is very strong (K_a > 10^4 M^{-1} at 333 K), while phosphate binding is much weaker (K_a = 34 ± 1 M^{-1} at 333 K). demonstrating a remarkable selectivity between sulfate and hydrogenphosphate at approximately neutral pH (at this pH, half of the phosphate anion will be present as H$_2$PO$_4^-$ and half as HPO$_4^{2-}$). Interestingly, the cage still shows significant sulfate binding in 1:1 pH = 9.0 tris-buffer:d$_6$-DMSO, despite the fact that the cage is significantly deprotonated under these conditions (Figure S66). While binding is not as strong as at neutral pH, an association constant of 970 ± 30 M^{-1} was determined at 333 K. Presumably, partial deprotonation of the urea N–H groups does not completely prevent binding in the cage cavity, and the polar solvent medium and high positive charge on the cage can overcome repulsion between the anionic urea group and the anion. Unfortunately, at this pH phosphate causes precipitation and so binding could not be quantified.

Conformational flexibility of cages, and effect of anion binding

At room temperature, both **cage^{urea}·Br$_6$** and **cage^{ph}·Br$_6$** have somewhat broadened ^{1}H NMR spectra, while **cage^{py}·Br$_6$** has a relatively sharp spectrum. We attribute this to conformational flexibility of the arms of the cage, particularly at the amide groups which can adopt either *anti* or *syn* conformations (Figure 4A), and where exchange between these conformations causes broadness of the ^{1}H NMR spectra. For both **cage^{urea}·Br$_6$** and **cage^{ph}·Br$_6$**, increasing the temperature to 333 K results in sharp spectra. In the case of **cage^{py}·Br$_6$**, favourable hydrogen bonds between amide

N–H groups and the pyridine nitrogen atom appear to favour the *syn-syn* conformation and thus minimise conformational flexibility. X-ray crystallographic studies support this hypothesis with crystal structures obtained of **cage**$^{ph\ 6+}$ and **cage**$^{urea\ 6+}$ containing both *syn-syn* and *syn-anti* amide/urea conformations. In contrast, two different crystal structures for **cage**$^{py\ 6+}$ show only the *syn-syn* conformation for all cage arms (see SI for all crystal structures).

In the interests of brevity, we will focus the rest of this discussion on **cage**$^{urea\ 6+}$ as this shows the most interesting anion binding properties. This cage has quite a broad ^{1}H NMR spectrum at 298 K that sharpens with increasing temperature; decreasing the temperature to 258 K results in a sharper, but lower symmetry spectrum (Figures S24 and S31). Sulfate binding at 298 K in 1:1 D_2O:d_6-DMSO results in significant broadening and evidence of a reduction in symmetry (Figure 3A). We attribute this reduction in symmetry in 1:1 D_2O:d_6-DMSO to sulfate "locking" the cage into the "buckled" conformation shown in Figure 4B where all urea groups are *syn-anti* and the cage has reduced symmetry caused by this arrangement. We note that all aromatic resonances show clear movement upon sulfate addition (Figure 2A) suggesting that spectral broadening is not caused solely by slow exchange between free cage and complexed cage. Binding in D_2O causes peak broadening but does not cause an obvious reduction in symmetry. We attribute this to weaker binding in pure water, resulting in the "locking" effect of the anion being less pronounced.

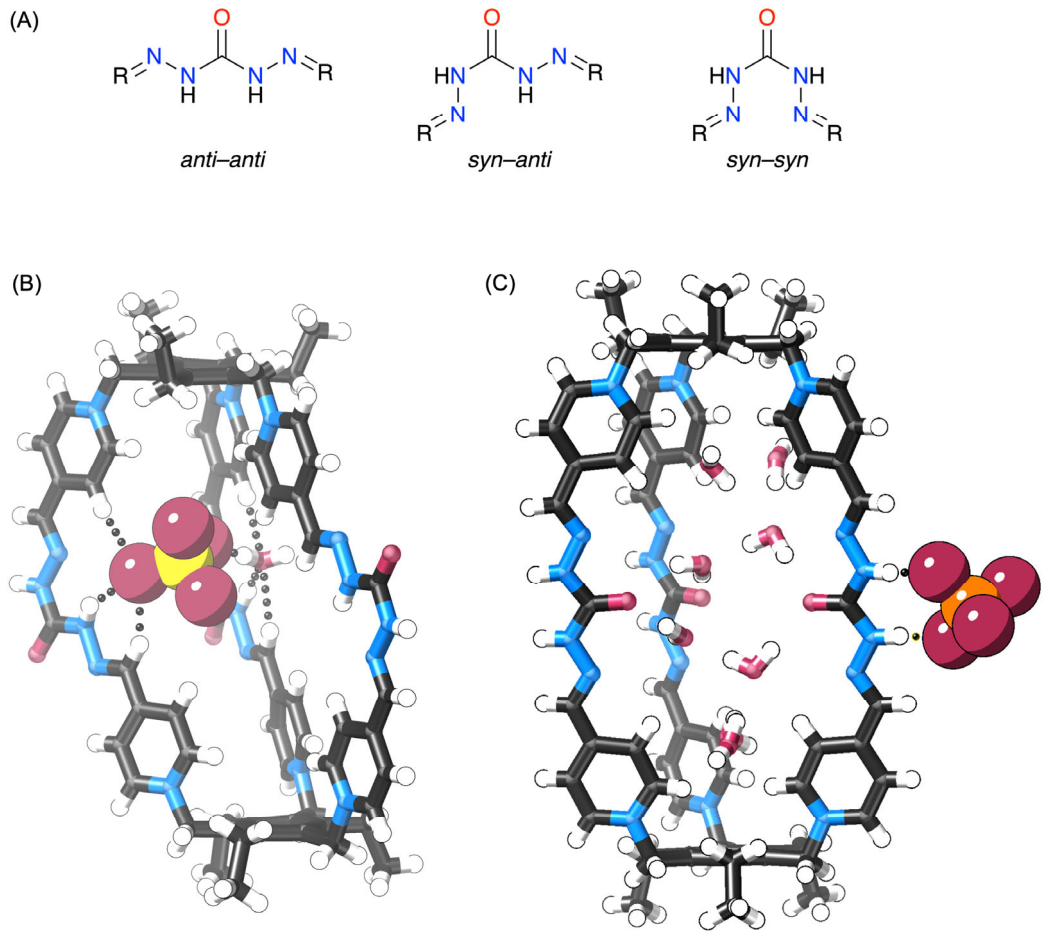

Figure 4. Urea geometries and their effect on cage conformations.

(A) Possible geometries of diiminourea groups.

(B) X-ray crystal structure of **cage**^{urea}·SO_4·$(NO_3)_4$. Disorder and nitrate anions are omitted for clarity. Dotted lines indicate a close contact shorter than 90% of the sum of the van der Waals radii of the H and O. PLATON-SQUEEZE was used.[73]

(C) X-ray crystal structure of **cage**^{urea}·$(H_nPO_4)_3$. The data are not of sufficient quality to determine if some urea groups are deprotonated, or the protonation state of the anions (see SI for full details). PLATON-SQUEEZE was used.[73]

We obtained single crystals of **cage**^{urea}·SO_4·$(NO_3)_4$ by slow evaporation of a solution of **cage**^{urea}·$(NO_3)_6$ and one equivalent of Na_2SO_4 in water and were able to characterise these by X-ray crystallography. Crystals of **cage**^{urea}·SO_4·Br_4 were almost identical but the data are quite poor (see SI). As shown in Figure 4B, the sulfate anion binds inside the cage, which adopts a buckled conformation with all urea groups adopting the *syn–anti* conformation. The anion receives three relatively short hydrogen bonds from a pyridinium, imine and urea group (H-O distances: 2.07 – 2.41 Å) as well as a short hydrogen bond from a water molecule that itself forms short hydrogen bonds with the cage. It is likely that the anion receives additional hydrogen bonds from further water molecules within the cage cavity, but unfortunately these could not be resolved and so the PLATON-SQUEEZE

routine[73] was used to include these solvent molecules in the refinement. Interestingly when crystals were obtained by adding an excess of HPO_4^{2-} to **cage**$^{urea\ 6+}$ in water, the cage adopts a linear conformation with all urea groups in an *anti–anti* conformation and the anion binding outside the cage (Figure 4C). While the quality of the data are not high enough to determine the protonation state of the anions or urea groups (see SI for further details), it is interestingly that this weakly-binding anion is located outside the cage cavity, while sulfate binds inside. Very small crystals were also obtained by adding KH_2PO_4 to **cage**^{urea}**·Br**$_6$ in water; while diffraction data collected from these using synchrotron radiation were too poor to allow full structure refinement, these crystals also have an *anti–anti* conformation and appear to have hydrogenphosphate anions located outside the cage cavity (see SI).

NMR spectroscopy and X-ray crystal structures both demonstrate that *anti–anti* and *syn–anti* arrangements of the urea group are possible in **cage**$^{urea\ 6+}$. A previous survey of the Cambridge Structural Database (CSD)[80] revealed that diarylurea groups have an overwhelming preference for the *anti–anti* conformation, with more than 99% of single crystal structures showing this conformation.[81] We surveyed the CSD for the diimino-urea motif present in **cage**$^{urea\ 6+}$ and found that only 35% of these structures adopt an *anti–anti* conformation with the remaining 65% adopting a *syn–anti* conformation (see SI). Further insight into the possible behaviour of **cage**$^{urea\ 6+}$ was obtained using computational calculations with the semi-empirical tight-binding method GFN2-xTB.[82] Molecular dynamics (MD) simulations were conducted for the 6^+ cage in implicit water starting from either a geometry where all urea groups had *syn–anti* conformations (such as that shown in Figure 4B), or where all urea groups had *anti–anti* conformations (such as that shown in Figure 4C). While the cage showed considerable flexibility in sampling different geometries, it was notable that *anti–anti* conformations were rarely seen, with *syn–anti* and *syn–syn* conformations occurring far more frequently.

Taken together, experimental data from NMR spectroscopy and X-ray crystallography in conjunction with computational calculations clearly demonstrate that these cages are dynamic and able to adopt numerous conformers in solution. It appears that this might contribute to the observed sulfate/hydrogenphosphate anion binding selectivity, and in the case of **cage**$^{urea\ 6+}$ allows the cage to contract to bind sulfate in a relatively small cavity locating the anion close to six cationic pyridinium rings. Future studies will investigate how further control over cage dynamics and conformation can be obtained with the aim of using this adaptive behaviour to gain conformation control over guest binding and reactivity.

CONCLUSIONS

We have reported a simple, high yielding, and scalable route to a small family of highly cationic hydrazone-based organic cages, and shown that these can be readily prepared on multigram scales. The resulting cages are highly robust and are stable to heating in water, DMSO or buffer solutions for extended periods. All three cages bind sulfate in highly polar DMSO/water solvent mixtures, and **cage**$^{urea\ 6+}$ binds this anion strongly in water, even at elevated temperatures and even in the presence of bromide anions, which are themselves favourably bound by the cage. High selectivity was obtained for sulfate over hydrogenphosphate anions in DMSO/aqueous buffer. The simple and modular nature of the synthesis suggests that a wide range of related cages should be readily accessible, including cages with greater water-solubility and those with cavities that can be tuned to bind a wide range of guest molecules.

EXPERIMENTAL PROCEDURES

Resource availability

Lead contact

Further information and requests for resources should be directed to the lead contact, Nicholas White (nicholas.white@anu.edu.au).

Materials availability

Requests for materials generated in this study should be sent to the lead contact, Nicholas White (nicholas.white@anu.edu.au).

Data and code availability

Crystallographic data are available from the Cambridge Crystallographic Data Centre (Reference codes: 2123004 – 2123006 and 2363366 – 2363373). Detailed experimental procedures, characterization data, and computational data are available in the SI.

Synthesis of cages

Solid **5·Br**$_3$ (1.00 equiv.) and the appropriate dihydrazide compound (1.50 equiv.) were heated to 80 °C in water for 24 – 72 hours during which time precipitates formed (reaction concentrations = 10, 40 and 50 mM in **5·Br**$_3$ for reactions to form **cage**$^{ph\ 6+}$, **cage**$^{py\ 6+}$ and **cage**$^{urea\ 6+}$, respectively). In the case of the reactions to form **cage**^{urea}**·Br**$_6$

and $\mathbf{cage^{ph}\text{-}Br_6}$, 2-bromopyridinium bromide (1.00 equiv., *i.e.* 33.3 mol% per reaction site) was also added. The cage precipitates were isolated by filtration, washed with water and then methanol, and then vacuum-dried. This gave pure $\mathbf{cage^{ph}\text{-}Br_6}$, $\mathbf{cage^{py}\text{-}Br_6}$ and $\mathbf{cage^{urea}\text{-}Br_6}$ in 67, 84 and 81% yields, respectively on 6.7 – 13.7 g scales.

SUPPORTING INFORMATION

Supporting Information is available online

ACKNOWLEDGMENTS

We thank Dr Michael Gardiner (Australian National University) for advice regarding X-ray crystallography. We are grateful to Dr Thomas Mason (Monash University), Prof. Ekaterina Izgorodina (Monash University), Prof. Michelle Coote (Flinders University) and Dr Andrew Tarzia (Politecnico di Torino) for helpful discussions. We thank the Australian Government for funding (RTP scholarship to EMF, Discovery Project DP230100190 to ALC and NGW). Parts of this research were carried out using the MX2 beamline[83] of the Australian Synchrotron and made use of the Australian Cancer Research Foundation detector. Parts of this research were undertaken with the assistance of resources from the National Computational Infrastructure (NCI Australia).

AUTHOR CONTRIBUTIONS

Conceptualisation: EMF and NGW; Formal analysis: all authors; Investigation: EMF, RJG, CCC, BRS and NGW; Resources: ALC and NGW; Writing – Original Draft: EMF and NGW; Writing – Review & Editing: all authors; Supervision: ALC and NGW; Project Administration: ALC and NGW; Funding Acquisition: ALC and NGW.

DECLARATION OF INTEREST

The authors declare no competing interests.

REFERENCES

(1) Kubik, S. Anion Recognition in Water. *Chem. Soc. Rev.* **2010**, *39* (10), 3648. https://doi.org/10.1039/b926166b.

(2) Langton, M. J.; Serpell, C. J.; Beer, P. D. Anion Recognition in Water: Recent Advances from a Supramolecular and Macromolecular Perspective. *Angew. Chem. Int. Ed.* **2016**, *55* (6), 1974–1987. https://doi.org/10.1002/anie.201506589.

(3) McNaughton, D. A.; Ryder, W. G.; Gilchrist, A. M.; Wang, P.; Fares, M.; Wu, X.; Gale, P. A. New Insights and Discoveries in Anion Receptor Chemistry. *Chem* **2023**, S2451929423003571. https://doi.org/10.1016/j.chempr.2023.07.006.

(4) Schmidtchen, F. P. Inclusion of Anions in Macrotricyclic Quaternary Ammonium Salts. *Angew. Chem. Int. Ed.* **1977**, *16* (10), 720–721. https://doi.org/10.1002/anie.197707201.

(5) Schiessl, P.; Schmidtchen, F. P. Binding of Phosphates to Abiotic Hosts in Water. *J. Org. Chem.* **1994**, *59* (3), 509–511. https://doi.org/10.1021/jo00082a001.

(6) Metzger, A.; Lynch, V. M.; Anslyn, E. V. A Synthetic Receptor Selective for Citrate. *Angew. Chem. Int. Ed.* **1997**, *36* (8), 862–865. https://doi.org/10.1002/anie.199708621.

(7) Kubik, S.; Goddard, R.; Kirchner, R.; Nolting, D.; Seidel, J. A Cyclic Hexapeptide Containing L-Proline and 6-Aminopicolinic Acid Subunits Binds Anions in Water. *Angew. Chem. Int. Ed.* **2001**, *40* (14), 2648–2651. https://doi.org/10.1002/1521-3773(20010716)40:14<2648::AID-ANIE2648>3.0.CO;2-#.

(8) Schmuck, C.; Schwegmann, M. A Molecular Flytrap for the Selective Binding of Citrate and Other Tricarboxylates in Water. *J. Am. Chem. Soc.* **2005**, *127* (10), 3373–3379. https://doi.org/10.1021/ja0433469.

(9) Yawer, M. A.; Havel, V.; Sindelar, V. A Bambusuril Macrocycle That Binds Anions in Water with High Affinity and Selectivity. *Angew. Chem. Int. Ed.* **2015**, *54* (1), 276–279. https://doi.org/10.1002/anie.201409895.

(10) Sudan, S.; Chen, D.; Berton, C.; Fadaei-Tirani, F.; Severin, K. Synthetic Receptors with Micromolar Affinity for Chloride in Water. *Angew. Chem. Int. Ed.* 2023, 62(9), e202218072, https://doi.org/10.1002/anie.202218072.

(11) Sivalingam, V.; Krishnaswamy, S.; Chand, D. K. A Template-Free Pd2L4 Cage with up to Nanomolar Affinity for Chloride in Aqueous Solutions. *Chem. Eur. J.* **2023**, *29* (33), e202300891. https://doi.org/10.1002/chem.202300891.

(12) Jing, L.; Deplazes, E.; Clegg, J. K.; Wu, X. A Charge-Neutral Organic Cage Selectively Binds Strongly Hydrated Sulfate Anions in Water. *Nat. Chem.* **2024**, *16*, 335-342. https://doi.org/10.1038/s41557-024-01457-5.

(13) Kubik, S.; Kirchner, R.; Nolting, D.; Seidel, J. A Molecular Oyster: A Neutral Anion Receptor Containing Two Cyclopeptide Subunits with a Remarkable Sulfate Affinity in Aqueous Solution. *J. Am. Chem. Soc.* **2002**, *124* (43), 12752–12760. https://doi.org/10.1021/ja026996q.

(14) Custelcean, R.; Williams, N. J.; Seipp, C. A. Aqueous Sulfate Separation by Crystallization of Sulfate–Water Clusters. *Angew. Chem. Int. Ed.* **2015**, *54* (36), 10525–10529. https://doi.org/10.1002/anie.201506314.

(15) Lee, S.; Chen, C.-H.; Flood, A. H. A Pentagonal Cyanostar Macrocycle with Cyanostilbene CH Donors Binds Anions and Forms Dialkylphosphate [3]Rotaxanes. *Nat. Chem.* **2013**, *5* (8), 704–710. https://doi.org/10.1038/nchem.1668.

(16) Prohens, R.; Martorell, G.; Ballester, P.; Costa, A. A Squaramide Fluorescent Ensemble for Monitoring Sulfate in Water. *Chem. Commun.* **2001**, No. 16, 1456–1457. https://doi.org/10.1039/B104172J.

(17) Zhou, H.; Zhao, Y.; Gao, G.; Li, S.; Lan, J.; You, J. Highly Selective Fluorescent Recognition of Sulfate in Water by Two Rigid Tetrakisimidazolium Macrocycles with Peripheral Chains. *J. Am. Chem. Soc.* **2013**, *135* (40), 14908–14911. https://doi.org/10.1021/ja406638b.

(18) Qin, L.; Wright, J. R.; Lane, J. D. E.; Berry, S. N.; Elmes, R. B. P.; Jolliffe, K. A. Receptors for Sulfate That Function across a Wide pH Range in Mixed Aqueous–DMSO Media. *Chem. Commun.* **2019**, *55* (82), 12312–12315. https://doi.org/10.1039/C9CC06812K.

(19) Li, J.; Clegg, J. K.; Wu, X. Charge-Neutral Urea Cages as Potent Synthetic Sulfate Receptors in Water. *ChemRxiv*, **2024**, https://doi.org/10.26434/chemrxiv-2024-fb64c.

(20) Langton, M. J.; Robinson, S. W.; Marques, I.; Felix, V.; Beer, P. D. Halogen Bonding in Water Results in Enhanced Anion Recognition in Acyclic and Rotaxane Hosts. *Nat. Chem.* **2014**, *6* (12), 1039–1043. https://doi.org/10.1038/nchem.2111.

(21) Mullaney, B. R.; Thompson, A. L.; Beer, P. D. An All-Halogen Bonding Rotaxane for Selective Sensing of Halides in Aqueous Media. *Angew. Chem. Int. Ed.* **2014**, *53* (43), 11458–11462. https://doi.org/10.1002/anie.201403659.

(22) Langton, M. J.; Marques, I.; Robinson, S. W.; Félix, V.; Beer, P. D. Iodide Recognition and Sensing in Water by a Halogen-Bonding Ruthenium(II)-Based Rotaxane. *Chem. Eur. J.* **2016**, *22* (1), 185–192. https://doi.org/10.1002/chem.201504018.

(23) A report by Gale and co-workers identified a macrocycle that displayed impressive selectivity in 60% water. This selectivity is believed to arise because the macrocycle assembles into nanotubes in solution, and these contain well-defined cavities: Wu, X.; Wang, P.; Turner, P.; Lewis, W.' Catal, O.; Thomas, D. S.; Gale, P. A. Tetraurea Macrocycles: Aggregation-Driven Binding of Chloride in Aqueous Solutions. *Chem*, **2019**, *5*, 1210-1222. https://doi.org/10.1016/j.chempr.2019.02.023.

(24) Park, C. H.; Simmons, H. E. Macrobicyclic Amines. III. Encapsulation of Halide Ions by in,in-1,(k + 2)-Diazabicyclo[k.l.m.]Alkane Ammonium Ions. *J. Am. Chem. Soc.* **1968**, *90* (9), 2431–2432. https://doi.org/10.1021/ja01011a047.

(25) Liu, Y.; Zhao, W.; Chen, C.-H.; Flood, A. H. Chloride Capture Using a C–H Hydrogen-Bonding Cage. *Science* **2019**, *365* (6449), 159–161. https://doi.org/doi:10.1126/science.aaw5145.

(26) Chen, Y.; Wu, G.; Chen, L.; Tong, L.; Lei, Y.; Shen, L.; Jiao, T.; Li, H. Selective Recognition of Chloride Anion in Water. *Org. Lett.* **2020**, *22* (12), 4878–4882. https://doi.org/10.1021/acs.orglett.0c01722.

(27) Bartl, J.; Kubik, S. Anion Binding of a Cyclopeptide-Derived Molecular Cage in Aqueous Solvent Mixtures. *ChemPlusChem* **2020**, *85* (5), 963–969. https://doi.org/10.1002/cplu.202000255.

(28) Wu, Y.; Zhang, C.; Fang, S.; Zhu, D.; Chen, Y.; Ge, C.; Tang, H.; Li, H. A Self-Assembled Cage Binding Iodide Anion over Halide Ions in Water. *Angew. Chem. Int. Ed.* **2022**, *61* (38), e202209078. https://doi.org/10.1002/anie.202209078.

(29) Xie, H.; Finnegan, T. J.; Liyana Gunawardana, V. W.; Pavlović, R. Z.; Moore, C. E.; Badjić, J. D. A Hexapodal Capsule for the Recognition of Anions. *J. Am. Chem. Soc.* **2021**, *143* (10), 3874–3880. https://doi.org/10.1021/jacs.0c12329.

(30) Xie, H.; Finnegan, T. J.; Liyana Gunawardana, V. W.; Xie, W.; Moore, C. E.; Badjić, J. D. A Double-Decker Cage for Allosteric Encapsulation of ATP. *Chem. Commun.* **2022**, *58* (40), 5992–5995. https://doi.org/10.1039/D2CC00927G.

(31) Samanta, J.; Tang, M.; Zhang, M.; Hughes, R. P.; Staples, R. J.; Ke, C. Tripodal Organic Cages with Unconventional CH–O Interactions for Perchlorate Remediation in Water. *J. Am. Chem. Soc.* **2023**. https://doi.org/10.1021/jacs.3c06379.

(32) Liu, X.; Liu, Y.; Li, G.; Warmuth, R. One-Pot, 18-Component Synthesis of an Octahedral Nanocontainer Molecule. *Angew. Chem. Int. Ed.* **2006**, *45* (6), 901–904. https://doi.org/10.1002/anie.200504049.

(33) Mal, P.; Schultz, D.; Beyeh, K.; Rissanen, K.; Nitschke, J. R. An Unlockable–Relockable Iron Cage by Subcomponent Self-Assembly. *Angew. Chem. Int. Ed.* **2008**, *47* (43), 8297–8301. https://doi.org/10.1002/anie.200803066.

(34) Tozawa, T.; Jones, J. T. A.; Swamy, S. I.; Jiang, S.; Adams, D. J.; Shakespeare, S.; Clowes, R.; Bradshaw, D.; Hasell, T.; Chong, S. Y.; Tang, C.; Thompson, S.; Parker, J.; Trewin, A.; Bacsa, J.; Slawin, A. M. Z.; Steiner, A.; Cooper, A. I. Porous Organic Cages. *Nat. Mater.* **2009**, *8*, 973. https://doi.org/10.1038/nmat2545 https://www.nature.com/articles/nmat2545#supplementary-information.

(35) Mastalerz, M.; Schneider, M. W.; Oppel, I. M.; Presly, O. A Salicylbisimine Cage Compound with High Surface Area and Selective CO2/CH4 Adsorption. *Angew. Chem. Int. Ed.* **2011**, *50* (5), 1046–1051. https://doi.org/10.1002/anie.201005301.

(36) Cantrill, S. J.; Rowan, S. J.; Stoddart, J. F. Rotaxane Formation under Thermodynamic Control. *Org. Lett.* **1999**, *1* (9), 1363–1366. https://doi.org/10.1021/ol990966j.

(37) Leigh, D. A.; Lusby, P. J.; Teat, S. J.; Wilson, A. J.; Wong, J. K. Y. Benzylic Imine Catenates: Readily Accessible Octahedral Analogues of the Sauvage Catenates. *Angew. Chem. Int. Ed.* **2001**, *40* (8), 1538–1543. https://doi.org/10.1002/1521-3773(20010417)40:8<1538::AID-ANIE1538>3.0.CO;2-F.

(38) Chichak, K. S.; Cantrill, S. J.; Pease, A. R.; Chiu, S.-H.; Cave, G. W. V.; Atwood, J. L.; Stoddart, J. F. Molecular Borromean Rings. *Science*, **2004**, *304* (5675), 1308–1312. https://doi.org/10.1126/science.1096914.

(39) Belowich, M. E.; Valente, C.; Smaldone, R. A.; Friedman, D. C.; Thiel, J.; Cronin, L.; Stoddart, J. F. Positive Cooperativity in the Template-Directed Synthesis of Monodisperse Macromolecules. *J. Am. Chem. Soc.* **2012**, *134* (11), 5243–5261. https://doi.org/10.1021/ja2107564.

(40) Hasell, T.; Chong, S. Y.; Jelfs, K. E.; Adams, D. J.; Cooper, A. I. Porous Organic Cage Nanocrystals by Solution Mixing. *J. Am. Chem. Soc.* **2012**, *134* (1), 588–598. https://doi.org/10.1021/ja209156v.

(41) Egleston, B. D.; Brand, M. C.; Greenwell, F.; Briggs, M. E.; James, S. L.; Cooper, A. I.; Crawford, D. E.; Greenaway, R. L. Continuous and Scalable Synthesis of a Porous Organic Cage by Twin Screw Extrusion (TSE). *Chem. Sci.* **2020**, *11* (25), 6582–6589. https://doi.org/10.1039/D0SC01858A.

(42) Givelet, C.; Sun, J.; Xu, D.; Emge, T. J.; Dhokte, A.; Warmuth, R. Templated Dynamic Cryptophane Formation in Water. *Chem. Commun.* **2011**, *47* (15), 4511. https://doi.org/10.1039/c1cc10510h.

(43) Hasell, T.; Schmidtmann, M.; Stone, C. A.; Smith, M. W.; Cooper, A. I. Reversible Water Uptake by a Stable Imine-Based Porous Organic Cage. *Chem. Commun.* **2012**, *48* (39), 4689. https://doi.org/10.1039/c2cc31212c.
(44) Caprice, K.; Pupier, M.; Kruve, A.; Schalley, C. A.; Cougnon, F. B. L. Imine-Based [2]Catenanes in Water. *Chem. Sci.* **2018**, *9* (5), 1317–1322. https://doi.org/10.1039/C7SC04901C.
(45) Lei, Y.; Chen, Q.; Liu, P.; Wang, L.; Wang, H.; Li, B.; Lu, X.; Chen, Z.; Pan, Y.; Huang, F.; Li, H. Molecular Cages Self-Assembled by Imine Condensation in Water. *Angew. Chem. Int. Ed.* **2021**, *60* (9), 4705–4711. https://doi.org/10.1002/anie.202013045.
(46) Alexandre, P.-E.; Zhang, W.-S.; Rominger, F.; Elbert, S. M.; Schröder, R. R.; Mastalerz, M. A Robust Porous Quinoline Cage: Transformation of a [4+6] Salicylimine Cage by Povarov Cyclization. *Angew. Chem. Int. Ed.* **2020**, *59* (44), 19675–19679. https://doi.org/10.1002/anie.202007048.
(47) Lauer, J. C.; Bhat, A. S.; Barwig, C.; Fritz, N.; Kirschbaum, T.; Rominger, F.; Mastalerz, M. [2+3] Amide Cages by Oxidation of [2+3] Imine Cages – Revisiting Molecular Hosts for Highly Efficient Nitrate Binding. *Chem. – Eur. J.* **2022**, *28* (51), e202201527. https://doi.org/10.1002/chem.202201527.
(48) Begato, F.; Penasa, R.; Wurst, K.; Licini, G.; Zonta, C. Combining Imine Condensation Chemistry with [3,3] Diaza-Cope Rearrangement for One-Step Formation of Hydrolytically Stable Chiral Architectures. *Angew. Chem. Int. Ed.* **2023**, *62* (30), e202304490. https://doi.org/10.1002/anie.202304490.
(49) Andrews, K. G.; Christensen, K. E. Access to Amide-Linked Organic Cages by in Situ Trapping of Metastable Imine Assemblies: Solution Phase Bisamine Recognition. *Chem. Eur. J.* **2023**, *29* (26), e202300063. https://doi.org/10.1002/chem.202300063.
(50) Jiao, T.; Wu, G.; Zhang, Y.; Shen, L.; Lei, Y.; Wang, C.-Y.; Fahrenbach, A. C.; Li, H. Self-Assembly in Water with N-Substituted Imines. *Angew. Chem. Int. Ed.* **2020**, *59* (42), 18350–18367. https://doi.org/10.1002/anie.201910739.
(51) Wu, G.; Wang, C.-Y.; Jiao, T.; Zhu, H.; Huang, F.; Li, H. Controllable Self-Assembly of Macrocycles in Water for Isolating Aromatic Hydrocarbon Isomers. *J. Am. Chem. Soc.* **2018**, *140* (18), 5955–5961. https://doi.org/10.1021/jacs.8b01651.
(52) Blanco-Gómez, A.; Fernández-Blanco, Á.; Blanco, V.; Rodríguez, J.; Peinador, C.; García, M. D. Thinking Outside the "Blue Box": Induced Fit within a Unique Self-Assembled Polycationic Cyclophane. *J. Am. Chem. Soc.* **2019**, *141* (9), 3959–3964. https://doi.org/10.1021/jacs.8b12599.
(53) Blanco-Gómez, A.; Neira, I.; Barriada, J. L.; Melle-Franco, M.; Peinador, C.; García, M. D. Thinking Outside the "Blue Box": From Molecular to Supramolecular pH-Responsiveness. *Chem. Sci.* **2019**, *10* (46), 10680–10686. https://doi.org/10.1039/C9SC04489B.
(54) Li, H.; Zhang, H.; Lammer, A. D.; Wang, M.; Li, X.; Lynch, V. M.; Sessler, J. L. Quantitative Self-Assembly of a Purely Organic Three-Dimensional Catenane in Water. *Nat. Chem.* **2015**, *7* (12), 1003–1008. https://doi.org/10.1038/nchem.2392.
(55) Wang, C.-Y.; Wu, G.; Jiao, T.; Shen, L.; Ma, G.; Pan, Y.; Li, H. Precursor Control over the Self-Assembly of [2]Catenanes via Hydrazone Condensation in Water. *Chem. Commun.* **2018**, *54* (40), 5106–5109. https://doi.org/10.1039/C8CC02599A.
(56) Chen, Q.; Chen, L.; Wang, C.-Y.; Jiao, T.; Pan, Y.; Li, H. Ultramacrocyclization via Selective Catenation in Water. *Chem. Commun.* **2019**, *55* (87), 13108–13111. https://doi.org/10.1039/C9CC06692F.
(57) Neira, I.; Blanco-Gómez, A.; Quintela, J. M.; Peinador, C.; García, M. D. Adjusting the Dynamism of Covalent Imine Chemistry in the Aqueous Synthesis of Cucurbit[7]Uril-Based [2]Rotaxanes. *Org. Lett.* **2019**, *21* (22), 8976–8980. https://doi.org/10.1021/acs.orglett.9b03377.
(58) Da Silva Rodrigues, R.; Luis, E. T.; Marshall, D. L.; McMurtrie, J. C.; Mullen, K. M. Hydrazone Exchange: A Viable Route for the Solid-Tethered Synthesis of [2]Rotaxanes. *New J. Chem.* **2021**, *45* (9), 4414–4421. https://doi.org/10.1039/D1NJ00388G.
(59) Cougnon, F. B. L.; Caprice, K.; Pupier, M.; Bauzá, A.; Frontera, A. A Strategy to Synthesize Molecular Knots and Links Using the Hydrophobic Effect. *J. Am. Chem. Soc.* **2018**, *140* (39), 12442–12450. https://doi.org/10.1021/jacs.8b05220.
(60) Lin, Z.; Emge, T. J.; Warmuth, R. Multicomponent Assembly of Cavitand-Based Polyacylhydrazone Nanocapsules. *Chem. Eur. J.* **2011**, *17* (34), 9395–9405. https://doi.org/10.1002/chem.201100527.
(61) Zheng, X.; Zhang, Y.; Wu, G.; Liu, J.-R.; Cao, N.; Wang, L.; Wang, Y.; Li, X.; Hong, X.; Yang, C.; Li, H. Temperature-Dependent Self-Assembly of a Purely Organic Cage in Water. *Chem. Commun.* **2018**, *54* (25), 3138–3141. https://doi.org/10.1039/C8CC01085D.
(62) Sharafi, M.; McKay, K. T.; Ivancic, M.; McCarthy, D. R.; Dudkina, N.; Murphy, K. E.; Rajappan, S. C.; Campbell, J. P.; Shen, Y.; Badireddy, A. R.; Li, J.; Schneebeli, S. T. Size-Selective Catalytic Polymer Acylation with a Molecular Tetrahedron. *Chem* **2020**, *6* (6), 1469–1494. https://doi.org/10.1016/j.chempr.2020.05.011.
(63) Wang, H.; Fang, S.; Wu, G.; Lei, Y.; Chen, Q.; Wang, H.; Wu, Y.; Lin, C.; Hong, X.; Kim, S. K.; Sessler, J. L.; Li, H. Constraining Homo- and Heteroanion Dimers in Ultraclose Proximity within a Self-Assembled Hexacationic Cage. *J. Am. Chem. Soc.* **2020**, *142* (47), 20182–20190. https://doi.org/10.1021/jacs.0c10253.
(64) Yang, M.; Qiu, F.; M. El-Sayed, E.-S.; Wang, W.; Du, S.; Su, K.; Yuan, D. Water-Stable Hydrazone-Linked Porous Organic Cages. *Chem. Sci.* **2021**, *12* (40), 13307–13315. https://doi.org/10.1039/D1SC04531H.
(65) Vestrheim, O.; Schenkelberg, M. E.; Dai, Q.; Schneebeli, S. T. Efficient Multigram Procedure for the Synthesis of Large Hydrazone-Linked Molecular Cages. *Org. Chem. Front.* **2023**, *10* (16), 3965–3974. https://doi.org/10.1039/D3QO00480E.
(66) Marcus, Y. Thermodynamics of Solvation of Ions. Part 5.—Gibbs Free Energy of Hydration at 298.15 K. *J. Chem. Soc. Faraday Trans.* **1991**, *87* (18), 2995–2999. https://doi.org/10.1039/FT9918702995.
(67) Duke, R. M.; O'Brien, J. E.; McCabe, T.; Gunnlaugsson, T. Colorimetric Sensing of Anions in Aqueous Solution Using a Charge Neutral, Cleft-like, Amidothiourea Receptor: Tilting the Balance between Hydrogen Bonding and Deprotonation in Anion Recognition. *Org. Biomol. Chem.* **2008**, *6* (22), 4089. https://doi.org/10.1039/b807579d.
(68) Brown, H. C.; McDaniel, D. H. The Base Strengths and Ultraviolet Absorption Spectra of the 2- and 3-Monohalopyridines. *J. Am. Chem. Soc.* **1955**, *77* (14), 3752–3755. https://doi.org/10.1021/ja01619a022.
(69) López, S. E.; Salazar, J. Trifluoroacetic Acid: Uses and Recent Applications in Organic Synthesis. *J. Fluor. Chem.* **2013**, *156*, 73–100. https://doi.org/10.1016/j.jfluchem.2013.09.004.
(70) Using $HBr_{(aq)}$ gave clean cages in better yields than those without addition of acid, but not as high as when 2-bromopyridinium bromide was used.
(71) Hunter, C. A.; Purvis, D. H. A Binary Quinone Receptor. *Angew. Chem. Int. Ed.* **1992**, *31* (6), 792–795. https://doi.org/doi:10.1002/anie.199207921.
(72) Alvarez, S. A Cartography of the van Der Waals Territories. *Dalton Trans.* **2013**, *42* (24), 8617–8636. https://doi.org/10.1039/c3dt50599e.
(73) Spek, A. L. PLATON SQUEEZE: A Tool for the Calculation of the Disordered Solvent Contribution to the Calculated Structure Factors. *Acta Crystallogr.* **2015**, *C71*, 9–18.
(74) Dolomanov, O. V.; Bourhis, L. J.; Gildea, R. J.; Howard, J. A. K.; Puschmann, H. OLEX2: A Complete Structure Solution, Refinement and Analysis Program. *J. Appl. Crystallogr.* **2009**, *42*, 339–341.
(75) *Bindfit*, accessed at supramolecular.org.
(76) Thordarson, P. Determining Association Constants from Titration Experiments in Supramolecular Chemistry. *Chem. Soc. Rev.* **2011**, *40* (3), 1305–1323. https://doi.org/10.1039/C0CS00062K.
(77) Ammer, J.; Nolte, C.; Karaghiosoff, K.; Thallmair, S.; Mayer, P.; de Vivie-Riedle, R.; Mayr, H. Ion-Pairing of Phosphonium Salts in Solution: C–H···Halogen and C–H···π Hydrogen Bonds. *Chem. Eur. J.* **2013**, *19* (43), 14612–14630. https://doi.org/10.1002/chem.201204561.
(78) Sommer, F.; Marcus, Y.; Kubik, S. Effects of Solvent Properties on the Anion Binding of Neutral Water-Soluble Bis(Cyclopeptides) in Water and Aqueous Solvent Mixtures. *ACS Omega* **2017**, *2* (7), 3669–3680. https://doi.org/10.1021/acsomega.7b00867.
(79) NanoAnalyze, TA Instruments, USA.
(80) Taylor, R.; Wood, P. A. A Million Crystal Structures: The Whole Is Greater than the Sum of Its Parts. *Chem. Rev.* **2019**, *119* (16), 9427–9477. https://doi.org/10.1021/acs.chemrev.9b00155.
(81) Luchini, G.; Ascough, D. M. H.; Alegre-Requena, J. V.; Gouverneur, V.; Paton, R. S. Data-Mining the Diaryl(Thio)Urea Conformational Landscape: Understanding the Contrasting Behavior of Ureas and Thioureas with Quantum Chemistry. *Tetrahedron* **2019**, *75* (6), 697–702. https://doi.org/10.1016/j.tet.2018.12.033.
(82) Bannwarth, C.; Ehlert, S.; Grimme, S. GFN2-xTB—An Accurate and Broadly Parametrized Self-Consistent Tight-Binding Quantum Chemical Method with Multipole Electrostatics and Density-Dependent Dispersion Contributions. *J. Chem. Theory Comput.* **2019**, *15* (3), 1652–1671. https://doi.org/10.1021/acs.jctc.8b01176.
(83) Aragao, D.; Aishima, J.; Cherukuvada, H.; Clarken, R.; Clift, M.; Cowieson, N. P.; Ericsson, D. J.; Gee, C. L.; Macedo, S.; Mudie, N.; Panjikar, S.; Price, J. R.; Riboldi-Tunnicliffe, A.; Rostan, R.; Williamson, R.; Caradoc-Davies, T. T. MX2: A High-Flux Undulator Microfocus Beamline Serving Both the Chemical and Macromolecular Crystallography Communities at the Australian Synchrotron. *J. Synchrotron Radiat.* **2018**, *25* (3), 885–891. https://doi.org/doi:10.1107/S1600577518003120.